MINI-RF RADAR CHARACTERISTICS OF THE CHANG'E-5 LANDING SITE IN OCEANUS PROCELLARUM. B. J. Thomson[1], J. D. Stopar[2], G. W. Patterson[3], S. S. Bhiravarasu[4], G. A. Morgan[5], and C. N. Nypaver[1], [1]Department of Earth and Planetary Sciences, University of Tennessee, Knoxville, TN, USA (bthom@utk.edu), [2]Lunar and Planetary Institute, Houston, TX, USA, [3]Johns Hopkins Applied Physics Laboratory, Laurel, MD, USA, [4]Space Applications Centre (ISRO), Ahmedabad, India, [5]Planetary Science Institute, Washington, DC, USA.

Introduction: In 2020, China's Chang'E-5 (CE5) lander returned the first lunar samples to Earth [1] since the Luna-24 mission in 1976 [2]. The CE5 landing site targeted a region in northern Oceanus Procellarum that exhibits some of the youngest crater retention ages on the mare [e.g., 1, 3, 4, 5]. Radiometric ages of the returned samples [6] provide a key calibration point to tie down the chronology of the Solar System, which is based on superposition relationships and the size-frequency distribution of impact craters [e.g., 7]. The majority of mare surfaces exhibit crater retention ages that cluster around 3.1–3.8 Ga [8], and most returned samples are similarly ancient. Younger tie points exist in the form of impact melts at small craters sampled by the Apollo astronauts, but there is a dearth of intermediate ages. Here we analyze Synthetic Aperture Radar (SAR) data of the CE5 site to search for potential sub-units within the mare basalt units mapped in the region. Similar approaches have investigated the stratigraphy of lava flow in Mare Imbrium [9] and inferred the presence of buried lava flow interfaces in low TiO_2 mare surfaces (i.e., those with low radar attenuation) [10]. The region was previously mapped as a single unit and named "*P*58" [8]. Additional work by [11] mapped the area as "*Em*4", with minor differences in boundaries. There is little compositional variation in VIS/NIR data across the deposits and have moderate TiO2 content [e.g., 5, 12, 13].

Data and methods: The Mini-RF (Miniature Radio Frequency) instrument is a side-looking radar instrument on the Lunar Reconnaissance Orbiter (LRO) spacecraft [14]. It is a dual frequency instrument that can collect hybrid polarity [15] radar images in the X or S bands (4.2 or 12.6 cm wavelengths, respectively). Mini-RF collected monostatic radar data from 2009–2011 [16], and has been operating in a bistatic configuration following a transmitter failure at the end of 2011 [17]. In a monostatic configuration, the single Mini-RF antenna is used to both transmit a radio signal and receive echoes off the lunar surface, while in a bistatic mode, a separate, Earth-based asset transmits a signal for which Mini-RF records the lunar echoes. Bistatic observations have not yet been acquired for the CE5 site, so the discussion below is limited to monostatic data [18]. These data have a spatial resolution of 15 m in azimuth and 30 m in range in Zoom mode. The side-looking geometry of imaging radar causes a topographic parallax where lower elevation surfaces are displaced outward in range. To correct for this effect, we used a digital elevation model (DEM) from the Lunar Orbiter Laser Altimeter (LOLA) instrument and SELENE Terrain Camera (TC) [19] to improve the geometric precision. A separate project is investigating residual errors in this topographic correction procedure [20].

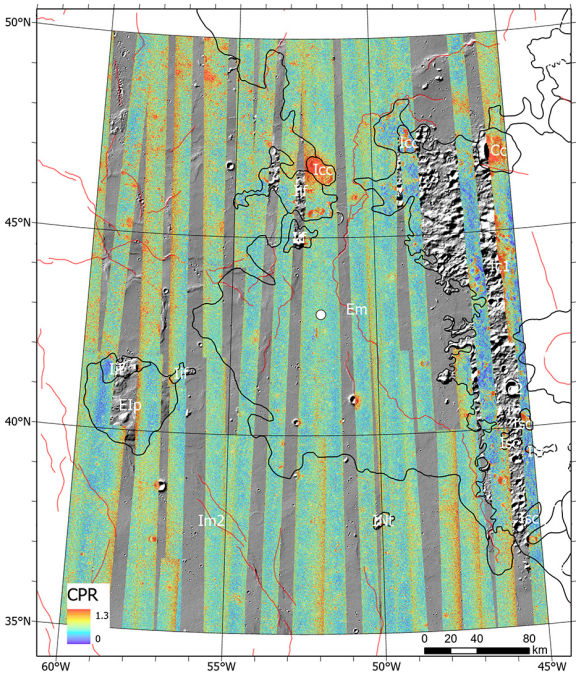

Figure 1. Mini-RF monostatic mosaic of CPR (circular polarization ratio) overlain on a topographic shaded relief map. The Chang'e-5 site is denoted by a white circle. Black and red lines are mapped geologic contacts and linear features from [17], respectively.

Results: A mosaic of monostatic Mini-RF S-band radar swaths is given in **Figure 1**. Geologic contacts from [21] are given with black lines; mapped linear features (including wrinkle ridges and rilles) are given with red lines. The CE5 site (indicated with a white circle in **Fig. 1**) lies with unit *Em*, an Eratosthenian mare unit (similar to unit *Em*4 of [11] and unit *P*58 of [8]). The contact between this unit and surrounding mare units, e.g., *Im2* to the south and east, is evident with the older, Imbrium-aged units exhibiting a higher density of small impact craters and higher overall circular polarization ratio (CPR) values. No evidence of

individual lava flows, flow fronts, or breakouts is evident in the radar data within unit *Em*/*P*58/*Em*4. The close spatial association of Rima Sharp, the longest sinuous rille system on the Moon (it is inferred to have flowed north to south [22]), suggests a possible genetic connection [13], but this remains indeterminate. Researchers have also proposed that CE-5 samples may be sourced by two different-aged rilles separated by several 100 Ma [13].

Conclusions: The lack of recognizable internal divisions in unit *Em*/*Em*4 evident with S-band radar suggests that it was rapidly emplaced within a narrow window of geologic time, a finding potentially in contrast to [12, 13] that favor a patchwork of eruptions over a broader time frame. Regolith gardening over ~2 Ga [5, 23] may have also muted and obscured such subtle traces, and crisscrossing of secondary craters and rays add noise as well (also complicating the record from which the crater size frequencies and surface ages are derived). This finding is consistent with optical observations that are indicative of internal compositional homogeneity [1, 3, 4, 11], making this unit an excellent Eratosthenian reference surface, adopting the sample age returned by CE5 as representative of the broader deposits [6].

Future work: Given recent success in recognizing mare subunits with bistatic data [24], we will be working to acquire X-band observations of the CE5 site in the future. L-band observations by the DFSAR instrument [25] on the Chandrayaan-2 spacecraft are also in the planning stages [26], which would provide views of different depths when searching for subsurface variations.

Acknowledgments: This work was supported in part by a contract to JHU/APL from NASA Goddard.

References: [1] Qian Y. et al. (2021) *EPSL*, *561*, 116855. [2] Barsukov V. (1977) *PLPSC*, *8*, 3303-3318. [3] Hiesinger H. et al. (2003) *JGR*, *108*. [4] Morota T. et al. (2011) *EPSL*, *302*, 255-266. [5] Jia B. et al. (2021) *JGR*, *126*, e2021JE006934. [6] Li Q.-L. et al. (2021) *Nature*, *600*, 54-58. [7] Neukum G. et al. (2001) *Space Sci. Rev.*, *96*, 55-86. [8] Hiesinger H. et al. (2011) *GSA Special Papers*, *477*, 1-51. [9] Morgan G.A. et al. (2016) *JGR*, *121*, 1498-1513. [10] Campbell B.A. et al. (2009) *GRL*, *36*, L22201. [11] Qian Y. et al. (2018) *JGR*, *123*, 1407-1430. [12] Giguere T.A. et al. (2021) *Icarus*, 114838. [13] Qian Y. et al. (2021) *GRL*, *48*, e2021GL092663. [14] Carter L.M. et al. (2017) *IEEE Trans. Geosci. Rem. Sen.*, *55*, 1915-1927. [15] Raney R.K. (2007) *IEEE Trans. Geosci. Rem. Sen.*, *45*, 3397-3404. [16] Cahill J.T.S. et al. (2014) *Icarus*, *243*, 173-190. [17] Patterson G.W. et al. (2017) *Icarus*, *283*, 2-19. [18] LRO Mini-RF Calibrated Level 2 Data (2008) PDS, doi:10.17189/1520649. [19] Barker M. et al. (2016) *Icarus*, *273*, 346–355. [20] Harris C.P. et al. (2002) *LPSC*, (this conference). [21] Fortezzo C.M. et al. (2020) *LPSC*, abstract #2760. [22] Hurwitz D.M. et al. (2013) *PSS*, *79*, 1-38. [23] Qian Y. et al. (2021) *GRL*, *48*, e2021GL095341. [24] Morgan G.A. et al. (2022) *LPSC*, (this conference). [25] Bhiravarasu S.S. et al. (2021) *Planet. Sci. J.*, *2*, 134. [26] Bhiravarasu S.S. et al. (2022) *LPSC*, (this conference).